AUTO-TERM DETECTION USING TIME-FREQUENCY ARRAY PROCESSING

Luke A. Cirillo

Communications & Signal Processing Group,
Curtin University of Technology,
GPO Box U1987, Perth 6845, Australia.
cirillo@ece.curtin.edu.au

Moeness G. Amin

Center for Advanced Communications,
Villanova University,
Villanova, Pa 19085.
moeness@ece.villanova.edu

ABSTRACT

The problem of nonstationary signal detection using antenna arrays is considered. A method for detection of source signal auto-term regions in the time-frequency plane is presented, based on spatial time-frequency distribution matrices. A general signal detection framework when using arbitrary time-frequency kernels is proposed and the trace of a whitened STFD matrix is used to form an appropriate test statistic. The expressions for the mean and variance of the statistic, necessary to evaluate the test, are provided. The detector performance using the Wigner-Ville distribution is investigated via simulated and theoretical results.

1. INTRODUCTION

Non-stationary signals such as frequency modulated (FM) and polynomial phase signals (PPS) arise in a number of fields including sonar, radar and telecommunications. Recently, the application of time-frequency (t-f) analysis to sensor array processing for non-stationary signals has received significant attention in the literature. The use of spatial time-frequency distribution (STFD) matrices in particular has emerged as a natural means for exploiting both the spatial diversity and t-f localization properties of non-stationary sources impinging on a sensor array.

Methods for blind source separation [1], direction-of arrival estimation [2, 3] and signal synthesis [4] have been proposed based on STFD processing. It has been shown that the relationship between the STFD of the sensor data and the time-frequency distributions (TFDs) of the sources is identical to that of the sensor data covariance matrix and the sources' correlation matrix. This key property permits direction finding and blind source separation to be performed *using the sources' t-f localization properties*. In a 'blind' scenario, no *a priori* knowledge of the source t-f localization can be assumed and must therefore be estimated [5, 6, 7].

This paper presents a general framework for detecting the locations in the t-f plane at which source signals exhibit a significant power concentration. The approach is a generalization of the auto-term detection technique considered in [6], based on thresholding array averaged TFDs using the Wigner-Ville kernel. It can be applied to arbitrary t-f kernels of Cohen's class [8]. Expressions for the mean and variance of a whitened array average using an arbitrary kernel are given. A signal detection framework is outlined and expressions for the detector performance are derived for the specific case of the pseudo Wigner-Ville distribution (PWVD). Performance of the detector is investigated for a range of model parameter values, including signal-to-noise ration (SNR), spatial separation of the sources and PWVD window length.

The work of Luke Cirillo has been partly supported by the Australian Telecommunications CRC. The work of Dr. Amin is supported by ONR, grant no. N00014-98-1-0176.

2. SIGNAL MODEL

We consider an m-element sensor array observing an instantaneous linear mixture of signals emitted from $d < m$ narrowband far-field sources. The vector $\mathbf{x}(n) \in \mathbb{C}^{m\times 1}$ represents a snapshot of the baseband array output at sampling instant n, which may be corrupted by an additive noise process $\mathbf{v}(n)$. The baseband array output model is

$$\mathbf{x}(n) = \mathbf{A}\mathbf{s}(n) + \mathbf{v}(n) \tag{1}$$

where $\mathbf{A} \in \mathbb{C}^{m\times d}$ is termed the mixing matrix and $\mathbf{s}(n) \in \mathbb{C}^{d\times 1}$ is a (deterministic) vector of the source signals. $\mathbf{A}$ is assumed to be of full column rank. We also assume that the sources have different localisation properties in the t-f plane and are 'uncorrelated' such that

$$\mathbf{R_s} \overset{\text{def}}{=} \lim_{T\to\infty} \frac{1}{T}\sum_{n=0}^{T-1} \mathbf{s}(n)\mathbf{s}^{\mathrm{H}}(n) = \mathbf{I}. \tag{2}$$

The noise process is assumed to be a complex circular white Gaussian process with variance σ_v^2 which is spatially and temporally uncorrelated. In the sequel a 'whitened' signal vector $\mathbf{z}(n) \in \mathbb{C}^{d\times 1}$ shall be considered

$$\mathbf{z}(n) = \mathbf{W}\mathbf{x}(n) = \mathbf{U}\mathbf{s}(n) + \mathbf{W}\mathbf{v}(n) \tag{3}$$

where $\mathbf{U}$ is a unitary matrix and $\mathbf{W}$ is termed the whitening matrix. We also define the signal part of the array output, $\mathbf{y}(n) = \mathbf{A}\mathbf{s}(n)$.

3. SPATIAL TIME-FREQUENCY DISTRIBUTIONS

A. Definitions

Consider two discrete-time sequences $x_1(n)$ and $x_2(n)$. The TFD in bilinear product form is defined according to

$$D_{x_1x_2}(n,\omega;\varphi) = \sum_{m,l=-\infty}^{\infty} \varphi(m,l)x_1(n+m+l)x_2^*(n+m-l)\mathrm{e}^{-\mathrm{j}2\omega l} \tag{4}$$

where $\varphi(m,l)$ is the kernel defining the distribution. The corresponding TFD in inner product form is given by

$$C_{x_1x_2}(n,\omega;\psi) = \sum_{m,k=-\infty}^{\infty} \psi(m,k)[x_1(n+m)\mathrm{e}^{-\mathrm{j}\omega m}][x_2(n+k)\mathrm{e}^{-\mathrm{j}\omega k}]^* \tag{5}$$

where $\psi(m,k) = \varphi((m+k)/2, (m-k)/2)$. The corresponding STFD matrices for a vector $\mathbf{x}(n)$ are defined according to

$$[\mathbf{D_{xx}}(n,\omega;\varphi)]_{ij} = D_{x_i x_j}(n,\omega;\varphi) \quad (6)$$

$$[\mathbf{C_{xx}}(n,\omega;\psi)]_{ij} = C_{x_i x_j}(n,\omega;\psi) \quad (7)$$

and for convenience the bilinear product form given by (6) shall be referred to as the STFD matrix in the sequel.

B. Statistical Properties

The sensor STFD matrix may be considered as a sum of three components

$$\mathbf{D_{xx}}(n,\omega;\varphi) = \mathbf{E} + \mathbf{F} + \mathbf{G}$$

where the matrices $\mathbf{E}$, $\mathbf{F}$ and $\mathbf{G}$ are defined as

$$\mathbf{E} \stackrel{\text{def}}{=} \mathbf{D_{yy}}(n,\omega;\varphi) \quad (8)$$

$$\mathbf{F} \stackrel{\text{def}}{=} \mathbf{D_{yn}}(n,\omega;\varphi) + \mathbf{D_{ny}}(n,\omega;\varphi) \quad (9)$$

$$\mathbf{G} \stackrel{\text{def}}{=} \mathbf{D_{nn}}(n,\omega;\varphi). \quad (10)$$

where the dependence on (n,ω,φ) has been dropped from the notation for convenience. Clearly the elements of matrices $\mathbf{F}$ and $\mathbf{G}$ are random due to the noise.

In the following $\text{Tr}\{\cdot\}$ denotes the trace of a matrix. The trace of the whitened STFD, $\text{Tr}\{\mathbf{D_{zz}}\}$, will be used for detection, and its statistical properties are considered below. Based on recent results by Stankovic [9], it can be shown that

$$\sigma_F^2 \stackrel{\text{def}}{=} \text{Var}\left[\text{Tr}\left\{\mathbf{WFW}^{\text{H}}\right\}\right] = 2\sigma_v^2 \sum_{i,j=1}^{d} \text{Re}\Big[\left(\mathbf{WW}^{\text{H}}\right) \odot \left(\mathbf{WC_{yy}}(n,\omega;\phi)\mathbf{W}^{\text{H}}\right)\Big]_{ij} \quad (11)$$

where $\odot$ denotes the element-wise matrix product and the kernel $\phi(m,k)$ is related to $\varphi(m,l)$ according to

$$\phi(m_1,m_2) = \sum_{k=-\infty}^{\infty} \varphi\left(\frac{m_1+k}{2}, \frac{m_1-k}{2}\right) \varphi^*\left(\frac{m_2+k}{2}, \frac{m_2-k}{2}\right). \quad (12)$$

Further, it can be shown that

$$\sigma_G^2 \stackrel{\text{def}}{=} \text{Var}\left[\text{Tr}\left\{\mathbf{WGW}^{\text{H}}\right\}\right] = \left\|\mathbf{WW}^{\text{H}}\right\|^2 \sigma_v^4 \sum_{m,l=-\infty}^{\infty} |\varphi(m,l)|^2. \quad (13)$$

The expected value, $\text{E}\left[\text{Tr}\left\{\mathbf{WFW}^{\text{H}}\right\}\right] = 0$, and

$$\mu \stackrel{\text{def}}{=} \text{E}\left[\text{Tr}\left\{\mathbf{WGW}^{\text{H}}\right\}\right] = \|\mathbf{W}\|^2 \sigma_v^2 \sum_{m=-\infty}^{\infty} \varphi(m,0). \quad (14)$$

Due to the noise properties

$$\text{Cov}\left[[\mathbf{F}]_{ij}, [\mathbf{G}]_{kl}\right] = 0,\ \forall\, i,j,k,l \in 1..m$$

which leads to

$$\sigma^2 \stackrel{\text{def}}{=} \text{Var}\left[\text{Tr}\left\{\mathbf{D_{zz}}(n,\omega;\varphi)\right\}\right] = \sigma_F^2 + \sigma_G^2. \quad (15)$$

Proof of results (11)-(15) are omitted here due to space limitations, and are to be published elsewhere.

4. SIGNAL DETECTION

A. Signal Detection Framework

The goal of the signal detection problem, is to determine the t-f locations at which the auto-source TFDs have significant peaks. Following the definition of a STFD matrix given in (6) and (7), we note that the auto-source distributions lie on the diagonal entries of the source STFD matrix. The signal detection problem can therefore be presented under a hypothesis testing framework, with statements of the null and alternate given respectively by

$$H_0: \quad \text{Tr}\{\mathbf{D_{ss}}(n,\omega;\varphi)\} = 0$$
$$H_A: \quad \text{Tr}\{\mathbf{D_{ss}}(n,\omega;\varphi)\} > 0.$$

Combining (3) and (8) yields:

$$\text{Tr}\left\{\mathbf{WEW}^{\text{H}}\right\} = \text{Tr}\left\{\mathbf{D_{ss}}(n,\omega;\varphi)\right\}$$

which motivates the use of the test statistic

$$T(n,\omega;\varphi) = \left(\text{Tr}\left\{\mathbf{D_{zz}}(n,\omega;\varphi)\right\} - \mu\right)/\sigma$$

where μ and σ are as defined in (14) and (15) respectively. The test is evaluated according to

$$T(n,\omega;\varphi) \underset{H_0}{\overset{H_A}{\gtrless}} \gamma(\alpha) \quad (16)$$

where γ is chosen according to a nominal level of significance (LOS), α, which corresponds to the probability of falsely detecting a signal component at a particular location of the t-f plane:

$$\Pr\left\{T(n,\omega;\varphi) > \gamma | H_0\right\} = \alpha. \quad (17)$$

Based on the asymptotic normality of the test statistic, we may calculate the threshold satisfying (17) as $\gamma(\alpha) = z(\alpha)$ where $z(\alpha)$ corresponds to the value exceeded by a normally distributed random variable with probability α.

The whitening transform, $\mathbf{W}$, and the noise variance, σ_v^2, are unknown parameters which must be estimated in practice, in order to evaluate the test according to (16). It is noted that the asymptotic distribution of $T(n,w;\varphi)$ remains unchanged provided consistent estimators of these parameters are used. Details for estimation of $\mathbf{W}$ and σ_v^2 can be found in, eg, [10].

We note that the expression for σ^2 given by (15) includes a signal dependent term, $\mathbf{C_{yy}}(n,\omega;\phi)$. However, as shown by Stankovic in [9], the peaks of this distribution lie along the signal auto-terms. For signals with well defined t-f signatures, the value of $\mathbf{C_{yy}}(n,\omega;\phi)$ should be approximately signal independent *under the null hypothesis*. This would allow evaluation of (16) for a wide class (eg polynomial phase) of nonstationary signals.

B. Pseudo Wigner-Ville Distribution

Details for signal detection using a particular TFD, the pseudo Wigner-Ville distribution (PWVD), are presented in this section. The kernel of the PWVD is given by

$$\varphi(m,l) = \delta(m)\text{rect}(l/L) \quad (18)$$

where $\mathrm{rect}(x) = 1,\ |x| < \frac{1}{2}$ and $\mathrm{rect}(x) = 0,\ |x| \geq \frac{1}{2}$. L denotes the (odd integer) window length parameter. Substituting (18) into (12) yields

$$\begin{aligned} C_{y_i y_j}(n,\omega;\phi) &= \sum_{m=-(L-1)/2}^{(L-1)/2} y_i(n+m)y_j^*(n+m) \\ &\approx L[\mathbf{A}\mathbf{A}^{\mathrm{H}}]_{ij} \end{aligned} \qquad (19)$$

where the approximation (19) follows from the uncorrelated assumption (2) and assuming a sufficiently large window length L. The mean and variance of $\mathrm{Tr}\,\{\mathbf{D_{zz}}(n,\omega;\varphi)\}$ under the null hypothesis, when using the PWVD, are given respectively by

$$\mu_W = \|\mathbf{W}\|^2 \sigma_v^2 \qquad (20)$$

$$\sigma_W^2 \approx L\sigma_v^2 \left(2\|\mathbf{W}\|^2 + \left\|\mathbf{W}\mathbf{W}^{\mathrm{H}}\right\|^2 \sigma_v^2\right). \qquad (21)$$

It is noted that the variance of $\mathrm{Tr}\,\{\mathbf{D_{zz}}(n,\omega;\varphi)\}$ is approximately signal independent (under assumption (2)) for the PWVD.

5. DETECTOR PERFORMANCE

In the following, detector performance is evaluated under a range of scenarios. The mixing system is generated according to the response of a uniform linear array (ULA) of sensors, with sensor spacing of half the carrier wavelength. The probability of detection is given by

$$P_d(\alpha, n, \omega, \varphi) = 1 - \Phi\left(\gamma(\alpha) - \frac{\mathrm{Tr}\,\{\mathbf{D_{ss}}(n,\omega;\varphi)\}}{\sigma}\right) \qquad (22)$$

where $\Phi(x)$ is the cumulative distribution function of the normal distribution. Two chirp signals ($d = 2$) are used to demonstrate the performance of the proposed detector.

A. Simulation

Simulation results are included to verify the theoretical results. The empirical probability of detection is evaluated along the t-f locations corresponding to the instantaneous frequency of the source signals. The empirical probability of false alarm is evaluated in the t-f regions which exclude the main lobes of the source signals. A 4 sensor ULA is considered, using 256 snapshots and a window length of $L = 65$ to compute the PWVD. The source signals have direction-of-arrival (DOA) given by $(0^o, 10^o)$.

Figure 1a shows the simulated and theoretical receiver operating characteristic (ROC) of the detector under a signal-to-noise ratio (SNR) of 0 dB. Figure 1b shows the achieved false alarm rate (P_{FA}) compared to the nominal level of significance. It is noted that the simulated values coincide closely with the theoretical both when using true and estimated values of parameters in the detector. For the simulated scenario a 97% probability of detection is achieved for a 5% probability of false alarm.

B. Discussion

From the expression for detector performance (22) it can be shown that the number of sensors, the angular separation of sources and the PWVD window length will have an effect on performance. This is demonstrated by evaluating (22) under a range of parameter values.

For a fixed nominal LOS of 5%, the probability of detection given by (22) is evaluated for a range of SNR from -15 to 10 dB and for source DOA of $(0^o, \Delta\theta)$ for $\Delta\theta$ varying in the range of 5^o to 35^o. All other parameters are as in the simulation example. As shown in Figure 2, the performance of the detector improves for increased spatial separation of the sources, up to approximately $\Delta\theta = 20^o$. After this point the performance is dictated by the value of SNR.

The effect of the number of sensors and the angular separation of sources on performance is illustrated in Figure 3. The results are obtain for an SNR of 0 dB. The probability of detection is evaluated with source DOAs of $(0^o, \Delta\theta)$ for $\Delta\theta$ varying in the range of 2^o to 26^o and the number of sensors varying from 3 to 15. The plot in Figure 3 demonstrates that for $\Delta\theta > 5^o$, performance is close to optimal for $m > 8$ sensors.

The influence of PWVD window length on performance is depicted in Figure 4. The results are obtained for $m = 5$ sensors and source DOAs of $(0, 10^o)$. The probability of detection is demonstrated for a range of SNR values from -20 to 10 dB and for PWVD window lengths of $L = 33, 45, 61$ and 127. The results indicate that detector performance is improved as the window length is increased. However, it is noted that the detector achieves this performance level only for $N - L + 1$ time-slices, and the performance will decrease at the rising and falling edges of the t-f distribution.

6. CONCLUSIONS

The problem of nonstationary signal detection is considered using t-f array processing. A method for detection of source signal auto-term regions on the time-frequency (t-f) plane has been presented, based on spatial time-frequency distribution (STFD) matrices. Detector performance using the Wigner-Ville distribution has been investigated via simulation and analysis. Results show that the detector performance increases with spatial separation of the sources, number of sensors and PWD window length. It is demonstrated that increasing the number of sensors or angular separation of sources only improved performance up to a point, beyond which the SNR and window length dominate the detector performance.

7. ACKNOWLEDGEMENTS

The authors would like to thank Prof. Abdelhak Zoubir for his valuable suggestions and comments on this work.

8. REFERENCES

[1] A. Belouchrani and M. G. Amin, "Blind source sepearation based on time-frequency signal representations," *IEEE Trans. Signal Processing*, vol. 46, no. 11, pp. 2888–2896, Nov. 1998.

[2] M. G. Amin, "Spatial time-frequency distributions for direction finding and blind source separation," *Proc. SPIE: Wavelet Applications IV*, vol. 3723, pp. 62–70, April 2000.

[3] Y. Zhang, W. Mu, and M. G. Amin, "Subspace analysis of time-frequency distribution matrices," *IEEE Trans. Signal Processing*, vol. 49, no. 4, pp. 747–759, Apr. 2001.

[4] Y. Zhang W. Mu and M. G. Amin, “Bilinear signal synthesis in array processing,” in *Proc. ICASSP*, Salt Lake City, Utah, May 2001.

[5] L. A. Cirillo, A. M. Zoubir, and M. G. Amin, “Selection of auto- and cross-terms for blind non-stationary source separation,” in *Proc. ISSPIT*, Cairo, Egypt, December 2001.

[6] L. A. Cirillo, A. M. Zoubir, N. Ma, and M. G. Amin, “Automatic classification of auto- and cross-terms of time-frequency distributions in antenna arrays.,” in *Proc. ICASSP*, Orlando, Florida, May 2002.

[7] L. Giulieri, N. Thirion-Moreau, and P.-Y. Arquès, “Blind source separation based on bilinear time-frequency representations: A performance analysis,” in *Proc. ICASSP*, Orlando, Florida, May 2002.

[8] L. Cohen, *Time-Frequency Analysis*, Prentice Hall, 1995.

[9] L. Stankovic, “An analysis of noise in time-frequency distributions,” *IEEE Signal Processing Letters*, pp. 286–289, September 2002.

[10] A. Belouchrani and M. Amin, “Source separation based on the diagonalization of a combined set of spatial time-frequency distributions,” *Proc. ICASSP*, April 1997.

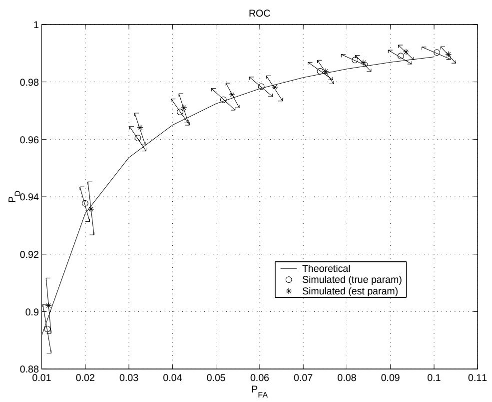

(a)

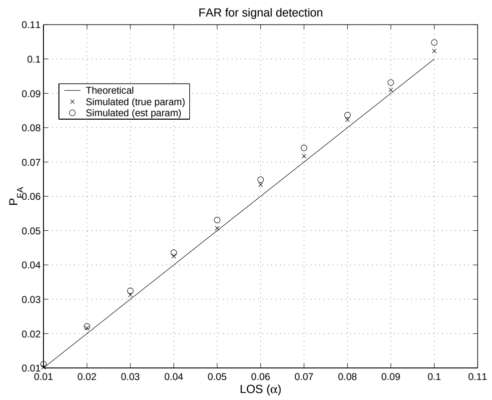

(b)

Fig. 1. (a) ROC of detector (with 99% Bootstrap confidence intervals for simulated values) and (b) P_{FA} of detector.

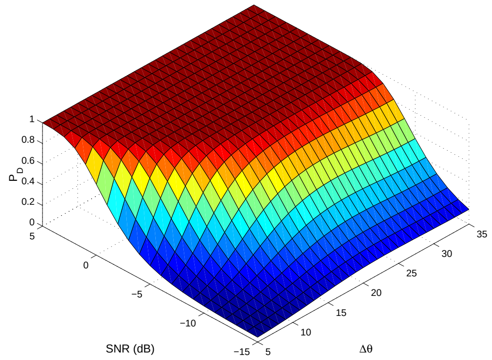

(b)

Fig. 2. Detector performance versus spatial separation of sources and SNR.

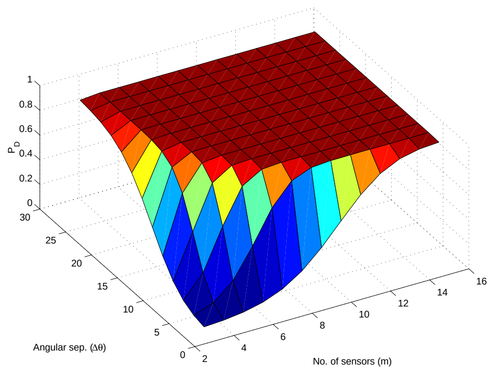

(b)

Fig. 3. Detector performance versus spatial separation of sources and number of sensors.

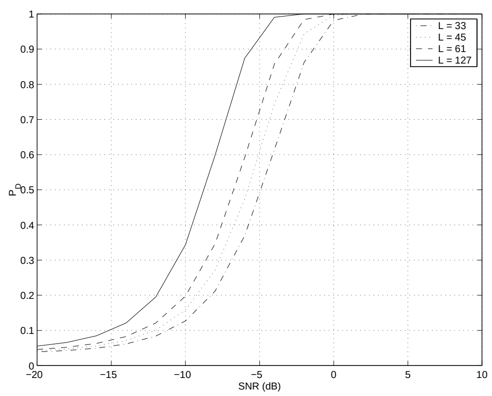

(b)

Fig. 4. Detector performance versus SNR for various PWVD window lengths.